

Confinement Induced First Order Crystallization Kinetics for the Poly(ethylene oxide) Block within A PEO-*b*-PB Diblock Copolymer Infiltrated within Alumina Nano-Porous Template

Rose Mary Michell,¹ Iwona Blaszczyk-Lezak,² Carmen Mijangos,²
Alejandro J. Müller*¹

Summary: We report homogeneous nucleation and first order crystallization kinetics for the PEO block within a PEO-*b*-PB diblock copolymer infiltrated within alumina nanopores. For the highly confined heterogeneity free PEO block nanodomains, the overall crystallization kinetics is dominated by nucleation and therefore becomes first order. The nucleation mechanism changes from heterogeneous nucleation for the PEO block within the uninfiltrated copolymer (since it has a composition with 79% PEO that conforms a percolated matrix) to homogeneous nucleation for confined and isolated heterogeneity free nanodomains.

Keywords: AAO templates; confinement; first order crystallization kinetics; homogeneous nucleation

Introduction

Crystallization under confinement has received much attention recently, since nanotechnology requires its understanding for future applications. Polymers can experience confinement in one, two or three dimensions and it is possible to find examples of confinement in droplet dispersions, blends, block copolymers, nanolayers and polymers infiltrated within inorganic templates.^[1–9]

In confined polymers, one of the following two situations can arise during solidification from the melt:

- (a) Crystallization occurs in a single crystallization step at much lower temperatures than the usual crystallization temperature (T_c) of the bulk polymer. This is encountered in systems charac-

terized by heterogeneity free domains, when the number of domains is several orders of magnitude higher than the number of heterogeneities present in the bulk polymer.

- (b) The crystallization occurs in several steps well spaced in temperature, i.e., fractionated crystallization.^[1,2] This situation occurs when the number of active heterogeneities is of the same order of magnitude than the number of domains, so that a significant population of domains still contain some type of heterogeneity.

In the case described in situation (a), the nucleation typically changes from a heterogeneous nucleation (present in the bulk polymer) to either homogeneous nucleation or surface nucleation of the domains (i.e., initiated at the surface of the domains or at the interface between the crystallizable domains and the matrix surrounding them). Surface nucleation is frequently encountered (although not often recognized in the literature^[9]), since it requires a lower free energy as compared with homogeneous nucleation.

¹ Grupo de Polímeros USB, Departamento de Ciencia de los Materiales, Universidad Simón Bolívar, Apartado 89000, Caracas 1080-A, Venezuela
Fax: (+58) 2129063388; E-mail: amuller@usb.ve

² Instituto de Ciencia y Tecnología de Polímeros, CSIC, Juan de la Cierva, 3, 28006 Madrid, Spain

In this paper, model confinement has been achieved by infiltrating a linear diblock copolymer with a crystallizable majority block (i.e., PEO-*b*-PB diblock copolymer) into nanoporous Alumina template. The crystallization of the PEO block changed from heterogeneous (in the bulk uninfiltreated sample) to homogeneous inside the nanopores. Additionally, the overall crystallization kinetics of the PEO block was determined. The crystallization kinetics order decrease from a third order to a first order time dependence as a consequence of confinement.

Experimental Part

Materials

A model poly(ethylene oxide) -*block*-poly(1,4-butadiene) diblock copolymer ($\text{Bd}_{21} - b - \text{EO}_{79}^{257}$) with a composition of 79 wt.% of PEO and 21 wt.% of PB and M_n equal to 257 kg/mol and a polydispersity index of 1.1 was employed.

Infiltration

The AAO templates employed in this work had an average diameter of 35 nm and pore lengths of approximately 100 μm . They were prepared by the two-step anodization method as reported elsewhere.^[10] The precursor film wetting method was used for infiltrating the $\text{Bd}_{21} - b - \text{EO}_{79}^{257}$ sample. The copolymer sample was heated to a temperature well above the melting point (T_m) during the infiltration (117.5 °C). Then the sample was annealed under a nitrogen atmosphere for 3 h to be sure that the copolymers will not degrade but, on the other hand, all pores will be infiltrated. After the infiltration process, the samples were quenched under ice-water and finally cleaned with the aid of a razor blade to remove any remaining copolymer on the surface.

Differential Scanning Calorimetry

Standard DSC Measurements

The infiltrated samples contained the precursor aluminum at the bottom of the template, plus the alumina template and

the infiltrated copolymer. The aluminum base was removed and 25 mg were employed consisting of just alumina template and the infiltrated copolymer. From these about 0.25–0.5 mg correspond to the copolymer sample according to TGA experiments. The samples were encapsulated in hermetically sealed 100 μL Aluminum pans.

A Diamond Perkin Elmer Instrument at 20 °C/min calibrated with zinc and indium under an ultra high purity nitrogen atmosphere was employed. For neat copolymer samples, the same scan rate was used and a mass of 5 mg.

Isothermal DSC Experiments

The isothermal crystallization kinetics employing DSC was performed by two methods: the conventional or “continuous isothermal crystallization”^[11] and the “isothermal step crystallization” technique.^[12]

The “continuous isothermal crystallization” experiments were performed to the un-infiltrated copolymer sample. After erasing the crystalline history of the samples by heating them for 3 min at 25 °C above the melting temperature, the samples were quickly cooled (at a controlled rate of 60 °C/min) to a crystallization temperature (T_c) at which the isothermal DSC scan was recorded. Experimental checks were performed to ensure that the sample did not crystallize during the cooling to T_c (by heating the samples immediately after reaching the corresponding T_c values and ensuring that no melting was observed, see ref.^[11]).

When the block copolymer sample is infiltrated within the alumina templates, the crystallization of the confined nanocylinders (inside the alumina nanopores) cannot be detected by standard isothermal crystallization experiments. The reason is that the heat evolved per unit time is too small to be detected by the calorimeter in isothermal mode.

Therefore, the isothermal crystallization of the block copolymer samples infiltrated in the alumina templates was determined with a technique employed previously with

block copolymer microphases termed “isothermal step crystallization”.^[12] A similar technique has also been used before by Galante et al.^[13] The procedure involved the following steps: (a) erasure of crystalline history by heating the sample to 25 °C above the melting temperature for 3 min; (b) fast cooling (at a controlled rate of 60 °C/min) down to T_c ; (c) the sample was held at T_c for a time t_c which was later increased in the subsequent steps; (d) heating at 20 °C/min from T_c to 25 °C above the melting temperature. The heat of fusion calculated from this DSC heating scan should correspond to the crystallization enthalpy of the crystals formed in step “c” at T_c for the specified crystallization time; (e) steps “a”–“d” were repeated employing the same T_c in step “b”, but increasing t_c . The final t_c was taken as the time the melting enthalpy in the subsequent heating scan did not change with respect to the previous one; (f) the whole process was repeated for different T_c temperatures.

Results and Discussion

Figure 1 shows the standard DSC results for neat and infiltrated diblock copolymer samples.

The melting and crystallization temperatures for the neat $\text{Bd}_{21}-b-\text{EO}_{79}^{257}$ diblock copolymer are within the expected range for PEO (see Table 1). This diblock copolymer exhibits a morphology of PB cylinders inside a PEO matrix.^[14] Since PEO is the matrix, nucleation is heterogeneous and the material crystallizes and melts in the typical range of PEO homopolymers.^[14]

On the other hand, once the copolymer is infiltrated in the AAO nanopores, confinement causes a dramatic reduction of the PEO block crystallization temperature. A similar behavior has been reported for PEO and other polymers that have been infiltrated in AAO templates, like PP, PE, sPS and PVDF.^[15–25] In the case of $\text{Bd}_{21}-b-\text{EO}_{79}^{257}$ diblock copolymer within a 35 nm AAO template, the crystallization temperature of the PEO block experience a reduction of 72.2 °C upon infiltration of the material. Such extreme supercoolings for PEO are characteristic of heterogeneity free nanodomains (considering the volume of the PEO phase inside the AAO pores).^[2,15,26,27] The number of nanopores in the templates is approximately 10 orders of magnitude higher than the number of active heterogeneities in the bulk

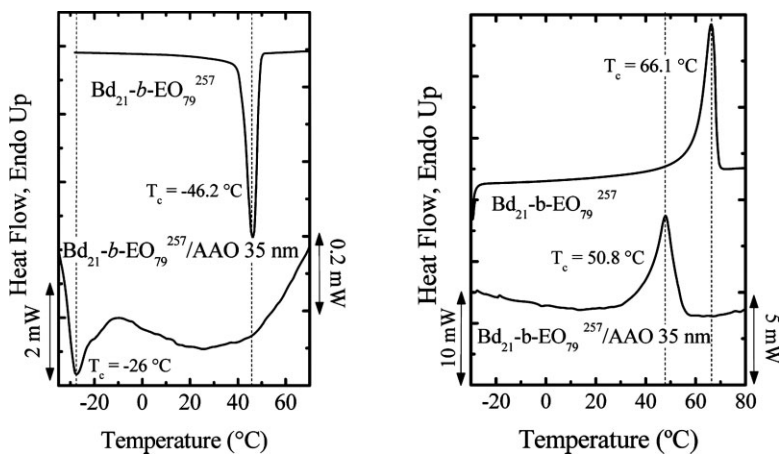


Figure 1.

DSC cooling (left) and heating (right) scans for the indicated samples. The y-axis scale on the left of the plots refers to the un-infiltrated neat materials, while that on the right to the AAO infiltrated materials. Data modified from ref.^[9].

Table 1.

Transition temperatures and enthalpies obtained by DSC standard heating and cooling scans.

Sample	T_c (°C)	ΔH_c (J/g)	T_m (°C)	ΔH_m (J/g)
Bd ₂₁ – b – EO ₇₉ ²⁵⁷	46.2	–111	66.1	122
Bd ₂₁ – b – EO ₇₉ ²⁵⁷ /AAO 35 nm	–26.0	–0.5*	50.8	0.6*

* These values are not normalized, because the exact weight of the polymer inside the nanopores is unknown.

PEO diblock copolymer, therefore, the number of clean MDs will be exceedingly higher than those with heterogeneities.

Müller et al.^[2] found an empirical relationship between the volume of the micro or nano domains and the crystallization temperature of PEO by analyzing a large amount of literature data:

$$T_c = -41.8 + 2.89 \log(v_d) \quad (1)$$

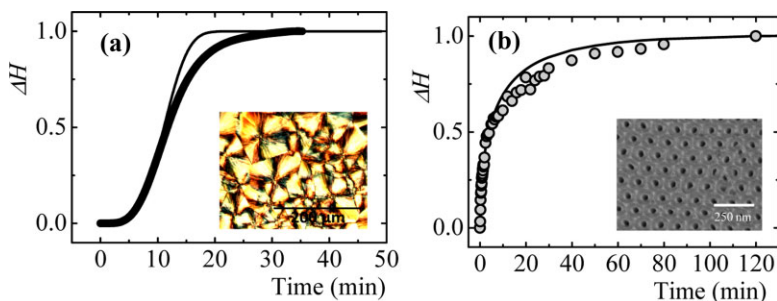
where T_c is the crystallization temperature of the PEO domains and v_d their average volume. In previous publications, we have employed this equation for the calculation of the crystallization temperature of infiltrated neat PEO and have found that its value correlates well with homogeneous nucleation of the PEO nanocylinders.^[9,15]

The morphology of the block copolymer may have changed with infiltration, as has been reported for other block copolymers in the literature.^[28–30] In any case, the volume occupied by the PEO block should be lower than the size of the nanopore (35nm), therefore the crystallization temperature for this system should be lower

than the crystallization temperature of an infiltrated PEO homopolymer. In fact the temperature reported in Table 1 for the PEO block within the infiltrated block copolymer is lower (–26 °C) than for neat infiltrated PEO reported by us using templates of identical pore volume (–22 °C^[9]). Hence, we believe that the nucleation of the PEO block nanodomains is homogeneous and not initiated at the interphases (i.e., at PEO-PB or PEO-AAO interphase).

If the nucleation of the infiltrated nanodomains is homogeneous, a first order crystallization kinetics would be expected. As detailed in the experimental part, in the case of the infiltrated block copolymer samples, the measurements of the overall isothermal crystallization kinetics were performed employing the DSC based step crystallization technique.

Figure 2 presents the results of the overall isothermal crystallization DSC experiments as the relationship between the relative degree of crystallinity ΔH and time for samples before and after

**Figure 2.**

Variation of the relative degree of crystallinity (expressed as relative ΔH values) with time for (a) Bd₂₁ – b – EO₇₉²⁵⁷ in the bulk ($T_c = 58$ °C) and (b) infiltrated within a 35nm AAO template ($T_c = -4$ °C). The insets show: (a) A polarized light optical micrograph of the Bd₂₁ – b – EO₇₉²⁵⁷ spherulites (formed by the PEO block major component) and (b) SEM micrograph of the AAO template (top view). The solid lines represent fits to the Avrami equation. Data modified from ref.^[9].

infiltration. In the case of un-infiltrated $\text{Bd}_{21}\text{-}b\text{-EO}_{79}^{271}$ the sample isotherm provided (at $T_c = 58^\circ\text{C}$) displays a typical sigmoidal shape, as expected for polymers free from confinement.^[9] It must be remembered that the PEO phase is a percolated matrix in this copolymer (with PB cylinders), hence it can develop spherulites (as shown in Figure 2 (a)). After infiltration a dramatic change is observed induced by confinement, since the curve corresponds to a simple exponential growth. This trend was observed for all the infiltrated samples at all the crystallization temperatures studied. A quantification of the order of the kinetics can be performed by fitting the results with the Avrami equation, closely following the procedure developed by Lorenzo et al.^[11] The Avrami equation^[31] can be written as:^[11]

$$1 - V_c(t - t_0) = \exp(-k(t - t_0)^n) \quad (2)$$

where V_c is the relative volumetric transformed fraction, t is the experimental time variable, t_0 is the induction time or the time at which the detection of crystallization starts, k is the overall crystallization rate constant and n is the Avrami index. Figure 3 shows typical Avrami plots for the data presented in Figure 2. All fittings were performed according to the recommendations given in ref.^[19] with a low conversion degree (up to 30%) and the correlation coefficients were always larger than 0.99.

The differences in overall crystallization kinetics shown in Figure 3 is striking since the Avrami coefficient (represented by the slope) changes from 3.8 to 0.6.

Müller et al.^[12] have argued that the Avrami exponent could be expressed by the addition of two terms:

$$n = n_n + n_{gd} \quad (3)$$

where n_n is related to nucleation and n_{gd} to growth dimensionality. The n_n term can have values ranging from 0 to 1 by considering that nucleation can be instantaneous or sporadic. Fractional values usually indicate that nucleation is not purely instantaneous or sporadic, but that it follows a certain characteristic kinetics in between these two extremes.

Figure 4(a) shows the changes in the Avrami index encountered upon infiltration for all the isothermal temperatures examined.

The values of the Avrami index for the PEO block within $\text{Bd}_{21} - b - \text{EO}_{79}^{257}$ are expected. The PEO block constitutes the percolated matrix of this diblock copolymer that contains PB cylinders. Figure 4(a) shows that the Avrami indexes increase from 2.5 at the lowest crystallization temperature to 3.8 for the highest, displaying an increasing trend with temperature. The results correspond to instantaneously nucleated spherulites at the low crystallization temperatures, if we approximate the value to $n = 3$. As the temperature is increased, the Avrami index also increases indicating that the spherulite nucleation

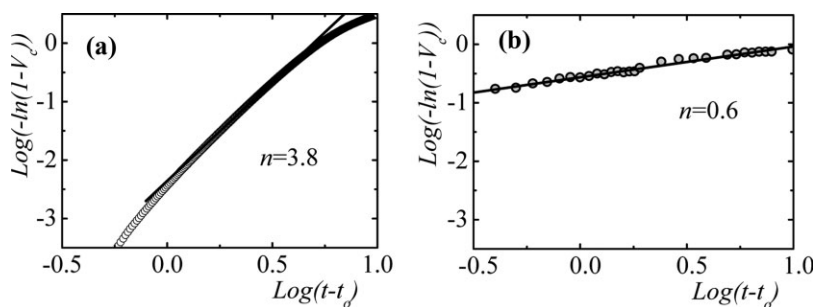


Figure 3.

Avrami plots for: (a) $\text{Bd}_{21} - b - \text{EO}_{79}^{257}$ in the bulk ($T_c = 58^\circ\text{C}$) and (b) infiltrated within a 35 nm AAO template ($T_c = -4^\circ\text{C}$). The solid lines represent fits to the Avrami equation.

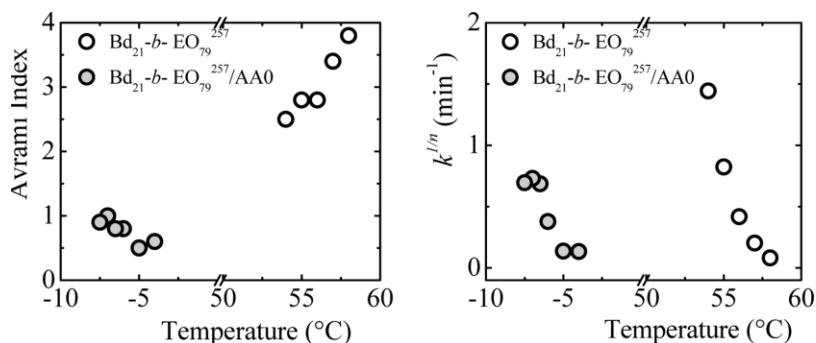


Figure 4.

a) Avrami index (n) values and b) $k^{1/n}$ versus temperature, for the block copolymer $Bd_{21}-b-EO_{79}^{257}$ before and after infiltration within a 35 nm AAO template.

is turning more sporadic with a limiting value of $n = 4$, as expected.

Upon infiltration, a dramatic drop in the Avrami index was obtained. The range of values for the infiltrated materials are roughly between 0.5 and 1 (each experiment was repeated 3 times). When the PEO block of the $Bd_{21}-b-EO_{79}^{257}$ diblock copolymer is confined into the AAO nanopores, the material crystallizes at extreme supercoolings, and the nucleation is most probably homogeneous, as argued above. Therefore, the rate determining step of the overall crystallization kinetics is probably the nucleation, since once a nucleus is produced inside one nanopore, crystal growth is extremely fast (see Figure 2). So, this would be equivalent to consider that $n_{gd} = 0$ and the Avrami equation would be only determined by the nucleation rate. Then when the nucleation is sporadic we would expect a first order kinetics or $n = 1$. First order kinetics have also been reported in the past for the crystallization of PEO spheres by Chen et al.^[27], Massa and Dalnoki-Veress^[32] and Reiter et al.^[33]

Shin et al. and Woo et al.^[17,23] studied the infiltration of a linear PE into AAO templates. They reported values of the Avrami index between 1.7 and 1.9, which does not correspond to the expected first order kinetics for truly isolated and confined heterogeneity free nanodomains. Additionally, the crystallization temperature range

employed is too high for homogeneous nucleation since the difference between T_c and T_g is of at least 100 °C. A surface nucleation mechanism is more plausible in their case. Duran et al.^[16] reported results on the infiltration of PP into alumina templates. They also obtained Avrami index values that are much higher than 1 (most values are between 2 and 2.5). It is difficult to understand these results but they do not conform to the expectation for homogeneous or surface nucleation.

Recently, we also reported first order kinetics for a PEO homopolymer confined within AAO templates that was able to nucleate homogeneously.^[9]

Another important parameter that can be obtained by fitting the data to the Avrami equation is k , the overall crystallization rate constant. One of the problems with k values is that the units of this parameter are expressed as time to the power n (e.g., min^{-n}). This singularity makes comparisons difficult to make if values of n are not constant. One way to overcome this difficulty is presented in Figure 4(b), where $k^{1/n}$ is used instead of k , so that the rate units are all in min^{-1} . In fact, the trends displayed by $k^{1/n}$ in Figure 4(b) are almost identical to those obtained by representing the inverse of the half-crystallization time as a function of T_c .^[9] Figure 4(b) shows that the infiltrated samples require a much larger supercooling to crystallize, a difference attributable to the higher energy barrier needed to activate homogeneous nuclei.

Conclusion

A clear change from heterogeneous to homogeneous nucleation of the PEO block corresponding to a $\text{Bd}_{21} - b - \text{EO}_{79}^{257}$ diblock copolymer has been obtained as a consequence of infiltrating the material into AAO nanopores. At least two distinct features support this conclusion: (a) The crystallization occurred at the maximum possible supercooling (considering the volume of the nanopores) and (b) The isothermal overall crystallization kinetics turned first order or lower ($n \leq 1$), since the kinetics inside the nanopores becomes dominated by the nucleation process.

Acknowledgments: We would like to thank Prof. Nikos Hadjichristidis and Dr. George Sakellariou for generously providing the PEO-*b*-PB diblock copolymer employed for AAO infiltration studies.

[1] H. Frensch, P. Harnischfeger, B. J. Jungnickel, in: "Multiphase polymers: blends and ionomers ACS symposium series 395", L. A. Utracki, R. A. Weiss, Eds., American Chemical Society, Washington 1989, p. 101–125.

[2] A. J. Müller, V. Balsamo, M. L. Arnal, *Adv. Polym. Sci.* **2005**, 190, 1.

[3] I. W. Hamley, *Adv. Polym. Sci.* **1999**, 148, 113.

[4] Y. Loo, A. Register, in: "Developments in Block Copolymer Science and Technology", I. W. Hamley, Ed., Wiley, New York 2004.

[5] R. V. Castillo, A. J. Müller, *Prog. Polym. Sci.* **2009**, 34, 519.

[6] A. J. Müller, V. Balsamo, M. L. Arnal, in: "Lecture notes in physics: progress in understanding of polymer crystallization", G. Reiter, G. Strobl, Eds., Springer, Berlin 2007, Vol. 714, pp 229–259.

[7] A. J. Müller, M. Arnal, A. T. Lorenzo, in: "Handbook of Polymer Crystallization", E. Piorkowska, G. Rutledge, Eds., Wiley, New York 2013.

[8] B. Nadan, J. Hsy, H. Chen, *Polym. Rev.* **2006**, 46, 143.

[9] R. M. Michell, I. Blaszczyk-Lezak, C. Mijangos, A. J. Müller, *Polymer* **2013**, 54, 4059.

[10] J. Martín, J. Maiz, J. Sacristan, C. Mijangos, *Polymer* **2012**, 53, 1149.

[11] A. T. Lorenzo, M. L. Arnal, J. Albuern, A. J. Müller, *Polym. Test.* **2007**, 26, 222.

[12] V. Balsamo, N. Urdaneta, L. Pérez, P. Carrizales, V. Abetz, A. J. Müller, *Eur. Polym. J.* **2004**, 40, 1033.

[13] M. Galante, L. Mandelkern, R. Alamo, A. Lehtinen, R. Paukkeri, *Therm. Anal.* **1996**, 47, 913.

[14] R. V. Castillo, M. L. Arnal, A. J. Müller, I. W. Hamley, V. Castelletto, H. Schmalz, V. Abetz, *Macromolecules* **2008**, 41, 879.

[15] R. M. Michell, A. T. Lorenzo, A. J. Müller, M. C. Lin, I. Blaszczyk-Lezak, J. Martín, C. Mijangos, *Macromolecules* **2012**, 45, 1517.

[16] H. Duran, M. Steinhart, B. Hans-Jürgen, G. Floudas, *Nano Lett.* **2011**, 11, 1671.

[17] K. Shin, E. Woo, Y. G. Jeong, C. Kim, J. Huh, K. W. Kim, *Macromolecules* **2007**, 40, 6617.

[18] M. C. Garcia-Gutiérrez, A. Linares, J. J. Hernández, D. R. Rueda, T. A. Ezquerro, P. Poza, P. R. Davies, *Nano Lett.* **2010**, 10, 1472.

[19] W. Hui, W. Wei, Y. Huang, C. Wang, Z. Su, *Macromolecules* **2008**, 41, 7755.

[20] J. L. Lutkenhaus, K. McEnnis, A. Serghei, T. P. Russell, *Macromolecules* **2010**, 43, 3844.

[21] M. Steinhart, P. G. Haissam, M. Prabhakaran, U. Gösele, *Phys. Rev. Lett.* **2006**, 97, 027801.

[22] M. Steinhart, S. Senz, R. B. Wehrspohn, U. Gösele, J. H. Wendorff, *Macromolecules* **2003**, 36, 3646.

[23] E. Woo, J. Huh, Y. G. Jeong, K. Shin, *Phys. Res. Lett.* **2007**, 98, 136103.

[24] H. Wu, W. Wang, Y. Huang, Z. Su, *Macromol. Rapid Commun.* **2009**, 30, 194.

[25] H. Wu, W. Wang, H. Yang, Z. Su, *Macromolecules* **2007**, 40, 4244.

[26] M. W. Massa, J. L. Carvalho, K. Dalnoki-Veress, *Eur. Phys. J.* **2003**, 12, 111.

[27] H. L. Chen, J. C. Wu, T. L. Lin, J. S. Lin, *Macromolecules* **2001**, 34, 6936.

[28] H. Xiang, K. Shin, T. Kim, S. I. Moon, T. J. McCarthy, T. P. Russell, *Macromolecules* **2005**, 38, 1055.

[29] P. Dobriyal, H. Xiang, M. Kazuy, T. P. Russell, *Macromolecules* **2009**, 42, 9082.

[30] G. J. A. Sevink, A. V. Zvelindovsky, J. G. E. Fraaije, H. P. Huinink, *J. Chem. Phys.* **2001**, 115, 8226.

[31] M. Avrami, *J. Chem. Phys.* **1941**, 9, 177.

[32] M. V. Massa, K. Dalnoki-Veress, *Phys. Rev. Lett.* **2004**, 92, 255509.

[33] G. Reiter, G. Castelein, J. Sommer, A. Röttele, T. Thurn-Albrecht, *Phys. Rev. Lett.* **2001**, 87, 226101.